

Article

The Mechanism of Changes in Hydraulic Properties of *Populus euphratica* in Response to Drought Stress

Duan Li ^{1,2}, Jianhua Si ^{1,2,*}, Xiaoyou Zhang ^{1,2}, Yayu Gao ^{1,2}, Huan Luo ^{1,2}, Jie Qin ^{1,2}
and Guanlong Gao ³

¹ Key Laboratory of Eco-hydrology of Inland River Basin, Northwest Institute of Eco-Environment and Resources, Chinese Academy of Sciences, Lanzhou 730000, China; liduan@lzb.ac.cn (D.L.); zhangxy@lzb.ac.cn (X.Z.); gaoyayu18@mails.ucas.ac.cn (Y.G.); huanluo@lzb.ac.cn (H.L.); qinjie18@mails.ucas.ac.cn (J.Q.)

² University of Chinese Academy of Sciences, Beijing 100049, China

³ Department of environment and resources, Shanxi University, Taiyuan 030006, China; gaoguanlong@sxu.edu.cn

* Correspondence: jianhuas@lzb.ac.cn

Received: 30 July 2019; Accepted: 10 October 2019; Published: 15 October 2019



Abstract: Stable hydraulic conductivity in forest trees maintains the survival of trees which contribute to productivity in forest ecosystems. Drought conditions break down this relationship, but the mechanisms are poorly known. To increase the understanding of the mechanism of hydraulic characteristics during drought, we determined hydraulic parameters in *Populus euphratica* Oliv. (*P. euphratica*) in a time-series of drought using a high-pressure flow meter. We found that *P. euphratica* could enhance hydraulic transport in severe drought stress under a threshold of soil water content. Drought-induced loss of hydraulic conductance could seriously impair water transport capacity. The soil water content of about 4.5% in the rhizosphere could lead to canopy mortality yet maintain live roots. Hydraulic conductance could be changed under drought stress as a consequence of changes in the anatomical structure and physiology. Furthermore, there was also a trade-off between hydraulic efficiency and safety. The consideration of hydraulic efficiency was first within the range of hydraulic safety limit. Once the hydraulic safety limit was reached, safety would be taken as the first consideration and hydraulic efficiency would be reduced. Research on the mechanism of hydraulic properties in riparian plants in arid areas provides a scientific basis for riparian forest restoration.

Keywords: *Populus euphratica*; riparian tree; hydraulic characteristic; threshold; water transport; trade-off; drought

1. Introduction

Drought constitutes one of the most critical challenges facing species and ecosystems. Drought resistance is related to water transport in plants and it affects the growth, development, and competitiveness of plant species [1]. Water transport in the xylem is related to plant drought resistance and forms the basis for maintaining survival [2,3]. Water transport in the xylem is the basis for maintaining the survival of terrestrial vascular plants [4]. Water is transported in the soil–plant–atmosphere continuum using hydraulic conductance in the xylem. Limitations in plant hydraulic conductance may undermine plant growth and lead to symptoms of decline. *Populus euphratica* Oliv. (*P. euphratica*) is a dominant riparian tree species in downstream oases of river basins in the arid inland region of China. The species plays a vital role in protecting biodiversity and maintaining riparian ecosystem functions of inland river basins [5,6]. The oasis environment fluctuates from wet to dry for riparian vegetation because of the different distance from the river and the seasonally artificial

discharge of water from the upper reaches of the river. Crown mortality of *P. euphratica* observed in many parts of the region during such an oasis environment raises concerns about the health of the oasis ecosystem. While the reasons for canopy mortality in *P. euphratica* are unclear, they may be related to hydraulic mechanisms that underlie plant adaptation to extremes of drought conditions.

Hydraulic functional traits act as critical factors affecting plant performance for the survival of the plant to sustain active hydraulic function in an adverse water environment [1,7]. It has been shown in numerous studies that plant responses to drought include changes in hydraulic conductance and increases in the likelihood of cavitation [8–11]. Drought stress increases water tension in the xylem, increasing the risk of cavitation in-plant transport systems [12]. Further, drought stress can affect xylem anatomical structure and physiological activity of plants. Moreover, hydraulic failure in some species is a reason for canopy mortality and even plant death in adverse water environment [13]. In order to deal with water shortage under drought conditions, plants strengthen their ability to obtain and transfer water by adjusting the anatomical structure and metabolic pathways [14,15]. Research on variability in hydraulic characteristics of trees in contrasting drought response strategies from anatomical and physiological changes can provide additional information on the coordination of hydraulic functional traits.

P. euphratica exhibits significant relationships among hydraulic traits, groundwater, and tree morphology [16–19]. For example, high vulnerability to xylem embolism was shown in both shoot and root; however, hydraulic variability underlying plant adaptation to a series of continuous drought conditions has not been addressed. Both drought and salt stress can cause a decrease in water potential in soil water and, consequently, in plant cells; water-loss in cells may lead to cell death. Previous studies on physiological and ecological responses (gas change, photosynthesis, and water use efficiency) to drought and salt stress suggested that *P. euphratica* had strong drought-resistant capability and salt-resistant characteristics [20–22]. Although *P. euphratica* evolved adaptive characteristics to cope with the presence of drought, understanding of the mechanism of changes in drought-induced hydraulic properties remains incomplete as to whether drought adaptation is related to variability in hydraulic architecture. It is known that the whole-plant hydraulic characteristics are determined by leaf, stem, and root hydraulic conductance when water moves through root, stem, and leaf conduits [23]. However, it is unclear whether water transport capacity is synchronized among plant organs in *P. euphratica* in extreme drought conditions. Therefore, the hydraulic characteristics of the root, shoots, and leaves need to be examined simultaneously to increase our understanding of the mechanisms of hydraulic characteristics, which could vary in changing the environment and may explain the presence of canopy mortality caused by water deficiency.

Our previous research showed that the leaf-specific hydraulic conductance of *P. euphratica* leaves increased significantly in dehydration treatments [16]. However, the effects of severe drought on the whole plant were not established. To research the mechanism of changes in hydraulic properties of each organ and the whole plant during drought, pot experiments were conducted to answer the following questions: (1) Do the hydraulic characteristics differ in *P. euphratica* in different duration of water stress? Is there a threshold of water content that leads to hydraulic failure for the plant or specific parts? (2) Does anatomical structure or physiology change in different duration of water stress? (3) How does the xylem adapt to drought stress through the trade-off between xylem efficiency and vulnerability to cavitation?

2. Materials and Methods

2.1. Study Sites

The lower reaches of the Heihe River Basin is located in the Alxa Plateau in northwestern China, characterized by a temperate desert climate. There is a vast natural forest belt, about 200 km long and 1 to 15 km wide across the region. *P. euphratica* is a dominant riparian plant with well-developed lateral roots. The *P. euphratica* forest, covering an area of about 1500 km², is one of the only three

existing *P. euphratica* forests in the world. Our study was conducted in the Alxa Desert Eco-hydrology Research Station of the Chinese Academy of Sciences (42°01' N, 100°21' E, altitude 883.54 m), which is about one hundred meters from the riverbank of the Heihe River (Figure 1). This area is one of the ultra-arid areas in China, where salinization and desertification reach severe levels. Local groundwater in the study area originates mainly from discharge in the middle and upper reaches of the river [18]. The average groundwater table is about 2.25 m. The average annual temperature is 8.2 °C. Annual precipitation is 38 mm, 75% of which occurs between June and August. Annual evaporation is more than 3390 mm, or 90 times more than the precipitation. The soil in this area is a fluvial and desert deposit, grayish-brown in color [24]. The soil water content in *P. euphratica* forests in this area ranged from 1.1% to 22.9% from the soil surface to a depth of 1.5 m. The study was conducted from April to August 2018. The highest and lowest temperatures during the study period were 38.67 °C and 3.46 °C, respectively. The average temperature, relative humidity, and vapor pressure deficit were 23.59 °C, 34.96%, and 2.17 kPa, respectively. Precipitation was 174.8 mm during this period.

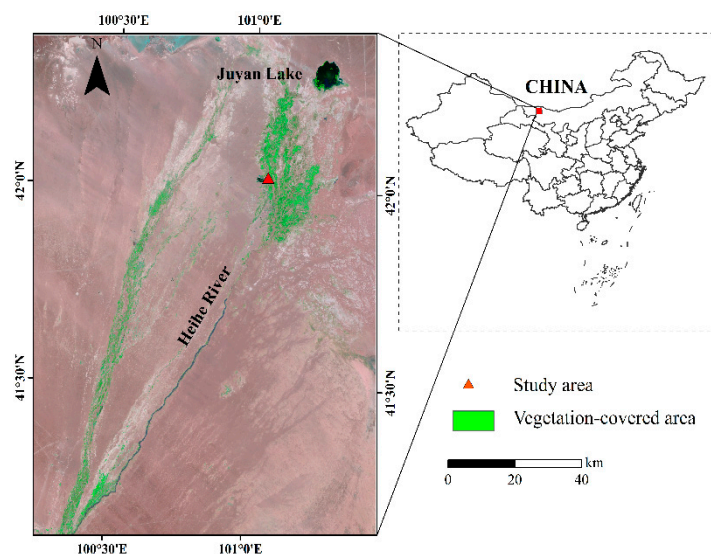


Figure 1. Remote sensing images of downstream oases in the Heihe River Basin in the arid inland region of China.

2.2. Plant Materials

Saplings of *P. euphratica* were planted in a nursery for about two years before they were transplanted into the pots. In early April 2018, one hundred saplings of *P. euphratica* were transplanted into the pots (about 33 cm in diameter and 25 cm in height generally) and placed outdoor in the natural environment. These saplings grew for more than three months with watering of 3 L every seven days according to a guide from the local forest farm of Ejina Banner before drought treatments. In late July 2018, we chose 20 healthy, straight, non-stressed, and well-growing samples from these saplings (around 40 cm in height and 0.45 cm in DBH) for drought treatments.

Drought treatments were imposed by suspending irrigation over the pots to reduce water supply. Meanwhile, a transparent plastic shed was placed over the pots on rainy days during the treatments to ensure controllable persistence of drought. Samples were assigned to five groups, each with four replications. Groups received one of the following drought treatments: Control check (CK; 0-days drought), 7-days treatment (drought period lasted for 7 days), 14-days treatment (drought period lasted for 14 days), 21-days treatment (drought period lasted for 21 days), and 28-days treatment (drought period lasted for 28 days). All drought treatments were carried out during 0–28 days. The starting day varied according to the drought treatments to ensure that the required drought duration met the same day for each group, which allowed us to avoid growth-induced differences in different drought treatments. Therefore, drought periods in different drought treatments started at 28, 21, 14, 7,

and 0 days before the ends of the treatments when the corresponding saplings of each group were not irrigated on the watering days (i.e., the plants were totally irrigated 4, 3, 2, 1, and 0 times for CK, 7-, 14-, 21-, and 28-days treatments, respectively). The saplings during the wet period in all the groups were still irrigated as before (Figure 2). The measurements for all the saplings were taken at once after the drought treatments.

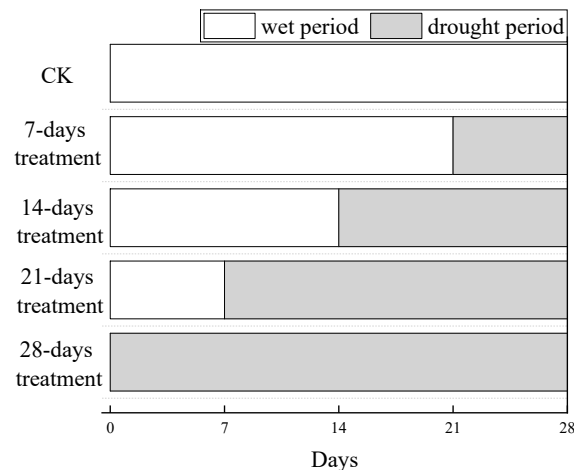


Figure 2. Drought periods in different treatments. CK: Control check.

2.3. Measurement of Hydraulic Conductance

Hydraulic conductance (k , $\text{kg s}^{-1} \text{MPa}^{-1}$) was determined with the water perfusion method and a high-pressure flow meter (HPFM-GEN3, Dynamax Inc., Houston, TX, USA) [25]. HPFM consisted of a device that presses distilled water into the root or shoot, and measured the corresponding flow rate; then, we obtained hydraulic conductance from the relationship between applied pressure and flow rate. Flow measurements in the root system were made with the HPFM operating in the “transient mode”, with pressure rapidly increasing from 0 to 500 kPa; values were then calculated from the slope of the linear regression. Flow measurements in the shoot system were made with the HPFM operating in the “steady mode” with stable pressure of 350 kPa until the rate of water flow entering the shoot stabilized. Each flow measurement sequence lasted about 10 min. The operating system corrected data for a reference temperature of 25 °C to compensate for changes in water viscosity caused by different measurement temperatures [25].

Water transport capabilities were measured as whole shoots/roots hydraulic conductance as above. The main stems were excised from the taproot at 3 cm above the soil surface. First, hydraulic conductance of whole shoots (k_{shoot}) and whole roots (k_{root}) was measured in the field when whole shoots were excised from roots. The ends of whole shoots and whole roots were attached to the instrument for testing to obtain k_{shoot} and k_{root} , respectively. The root system was for the in-situ measurement while it remained in the soil and the distilled water was pushed down from the cut end of the root protruded from the soil. Then, leaves were removed to obtain new hydraulic conductance values—leaf hydraulic conductance (k_{leaf}), which was an integral measure of total-leaf transpiration flow-paths from the stem–leaf junction to evaporation points [26]. Hydraulic conductance of leaves (k_{leaf}) was calculated based on Ohm’s law hydraulic pressure analog, as follows [27]:

$$k_{\text{leaf}} = (k_{\text{shoot}}^{-1} - k_x^{-1})^{-1} \quad (1)$$

where k_{shoot} was the hydraulic conductance of whole shoots, and k_x was the hydraulic conductance of bare shoots.

Hydraulic segmentation represented by hydraulic resistance ratio (R, %) can reflect the hydraulic contribution of each part. This was calculated with hydraulic resistance ($1/k$) of each part as a percentage

of the total. Measured hydraulic conductance was adjusted for total leaf area to obtain leaf-specific hydraulic conductance (k_l , $\text{kg s}^{-1} \text{MPa}^{-1} \text{m}^{-2}$), expressed as hydraulic conductance per area. Besides this, a calculation method for total leaf area is described below.

2.4. Total Leaf Area

To determine leaf area, several fresh leaves from four saplings of five groups were pasted on grid paper and their outline was drawn. The number of grids in which the leaf covered > 50% of the grid area was counted. Then, the leaf area was calculated by multiplying the number of grids by the area of a single grid. These leaves were frozen in liquid nitrogen for further study after leaf area determination. Additionally, five to ten more leaves from four saplings of five groups were obtained from the saplings, and their leaf area was determined as above. These leaves were washed, dried at 80 °C, and then weighed on an electronic balance to obtain biomass and specific leaf weight (leaf area/biomass) per sapling [28]. The area of the remaining leaves was determined after collecting, drying at 80 °C, and weighing, then assuming the same SLW for each individual sapling. Finally, the total leaf area of each sapling was determined by adding the leaf area of all leaves. Dried leaves were stored in envelopes for later ion content determination.

2.5. Malondialdehyde (MDA) Content Determination

Leaves from four saplings of five groups frozen in liquid nitrogen were used for malondialdehyde (MDA) content analysis. MDA is a physiological trait which determines possible oxidative stress which could reflect stress-induced damage on cell membranes [29]. The MDA content was assayed using commercially-available kits (Comin Biotechnology Co., Ltd., Suzhou, China). 0.1 g was accurately weighed by the analytical balance after samples were ground in liquid nitrogen and then homogenized in 1 mL of 50 mM phosphate buffer (pH 7.8). The homogenate was centrifuged at 12,000 rpm for 15 min at 4 °C and the resulting supernatant was used to measure MDA content with thiobarbituric acid chromatometry (TBA).

2.6. Ion Content Determination

In the laboratory, dried leaves were ground for further experiments. Dried leaves 0.25-g subsamples were digested in 4 mL high purity concentrated HNO_3 in ceramic crucibles on a hotplate at 200 °C for 1 h to allow evaporation to almost dryness. The crucibles were transferred to a muffle furnace, and samples were ashed at 450–500 °C for 8 h. Then, the residue was completely dissolved in 4 mL HCl. The digest solution was made up to 10 mL with deionized water and stored until K^+ , Mg^+ , and Ca^+ content determination using Inductively Coupled Plasma–Optical Emission Spectrometer (Optima 8000, PerkinElmer Inc., Waltham, MA, USA).

2.7. Soil Water Content Determination

After obtaining hydraulic measurements, pots were emptied of all soil with roots, and three aluminum boxes (about 50 mm in diameter and 30 mm in height) per treatment were filled with rhizosphere soil to measure soil moisture content. Soil water content was determined as $(M_w - M_d)/(M_d - M) \times 100\%$, where M_d was weight of dry soil with container after oven-drying at 105 °C to a constant weight, M_w was the weight of wet soil with the container, and M was the weight of the empty container.

2.8. Xylem Anatomy

A section of each main stem, leaf, and taproot about 3 cm long was cut off after soil water content determination, then cleaned and stored in a plastic bottle with a formaldehyde–acetic acid–70% ethanol fixative (5:5:90, v:v:v) for structural observations.

The samples were taken out of the fixative, and were then cut into 3–5 mm lengths, dehydrated through a graded ethanol series (50%, 70%, 85%, 95%, and 100%), and embedded in paraffin. Then, 16 µm-thick transverse section of each sample was cut using a sliding microtome, mounted on glass slides with glyceride, stained with safranin 0.1% (weight/volume) and 0.5% astra blue for 3 min, mounted on microscope slides, and fixed with quick-dry glue for light-microscopic observation. Images of the prepared transverse cuts were taken using a digital camera attached to an Olympus BX50 light microscope (Olympus CX31, Olympus America Inc., Center Valley, PA, USA).

Mature vessels with a red color could be seen when the samples were stained with safranin 0.1% and 0.5% astra blue. The mature vessels close to the phloem of the xylem transverse sections were chosen to analyze the anatomical features. The xylem transverse section was divided into four quarters, and a minimum of 30 vessels per quarter per treatment was measured for each segment to obtain the diameter of each vessel (d). The multiple sites could ensure the representativeness of the general anatomical features of the xylem transverse section. The total number of the vessels chosen in the four quarters of each xylem transverse section was more than 120, which was large enough to reflect the anatomical features of the vessels [30]. Anatomical features were measured using image analysis software Image J. The vessel hydraulic diameter (d_h) was calculated from the formula:

$$d_h = \sum d^5 / \sum d^4 \quad (2)$$

The parameter d_h weights vessel diameters by their hydraulic contribution, which is a function of the diameter d to the fourth power [31]. Besides, the parameter “thickness-to-span ratios” $(t/b)^2$, used as anatomical proxies for vessel wall reinforcement, were also calculated, where b was the vessel diameter and t was the double thickness of vessel wall [32,33]. Wall thickness was measured on tangential walls that did not contain pits.

Inter-tracheid pits of the saplings were studied with ultrahigh-resolution thermal field emission scanning electron microscope and energy spectrometer (MLA650, FEI Inc., Oregon, OR, USA). Samples for SEM were cut into 5–10 mm lengths, split in half, and dehydrated in a graded series of ethanol followed by acetone, and then dried with automated critical point dryer (EM CPD300, Leica Microsystems Inc., Germany). The specimens were mounted on stubs, sputter-coated with platinum, and examined with a digital scanning electron microscope at 5–10 kV. Pictures were scanned and analyzed with standard image analysis software.

2.9. Data Treatment and Statistical Analysis

Analysis of variance (ANOVA) was performed to test for differences in hydraulic values, the parameters of xylem anatomy, total leaf area, MDA content, ion content, and soil water content among different drought treatments. We used the least significant difference test (LSD) based on post hoc means. Pearson Product Moment Correlation was selected to test the statistical significance of correlations. A probability value of $p < 0.05$ was used to indicate statistically significant differences. Data were presented as means with standard error and statistically analyzed using SPSS 19.0 (IBM Corp., New York, NY, United States). Figures were plotted using Origin 8.0 (OriginLab Corp., Northampton, MA, USA).

3. Results

3.1. Characteristics of Hydraulic Conductance

Absolute hydraulic conductance in whole roots gradually increased with drought duration from 0 to 14 days, and then increased significantly to $1.51 \times 10^{-4} \text{ kg s}^{-1} \text{ MPa}^{-1}$, or 1.78 times the value in CK treatment (no drought) on day 21. Subsequently, absolute hydraulic conductance significantly decreased to 25% of the value in CK treatment when drought stress lasted for 28 days. Absolute hydraulic conductance of whole shoots gradually increased with drought duration from 0 to 14 days, decreased significantly after 21 days, and was $4.34 \times 10^{-6} \text{ kg s}^{-1} \text{ MPa}^{-1}$, or about 46.4% lower than in the CK treatment after 21 days. There was a loss of about 85.2% in hydraulic conductance than in the CK treatment after 28 days. The trend in leaves was the same as that in whole shoots. The final value of absolute hydraulic conductance was $3.07 \times 10^{-5} \text{ kg s}^{-1} \text{ MPa}^{-1}$ or about half of that in CK treatment when drought lasted for 28 days (Figure 3A).

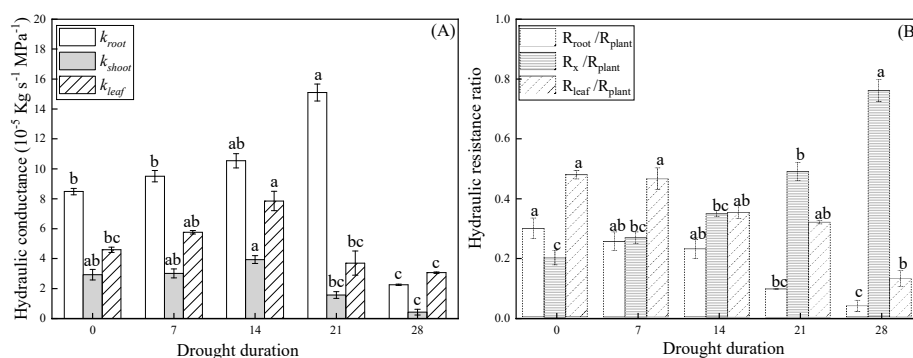


Figure 3. Changes in hydraulic conductance (A) and hydraulic resistance ratio (B). (A): k_{root} (open bars) indicate hydraulic conductance of whole roots, k_{shoot} (light-shaded bars) indicate hydraulic conductance of whole shoots, k_{leaf} (hatched bars) indicate hydraulic conductance of leaves. (B): R_{root}/R_{plant} (open bars) indicate hydraulic resistance ratio of whole roots to whole plant, R_x/R_{plant} (light-shaded bars) indicate hydraulic resistance ratio of bare shoots to whole plant, R_{leaf}/R_{plant} (hatched bars) indicate the resistance ratio of leaves to the whole plant. Different lower-case letters denote significance levels based on ANOVA (Analysis of variance) post hoc means with LSD (least significant difference test) analysis ($p < 0.05$). Data are means with standard error.

There was a gradual decline from 30% to 4% in hydraulic resistance of roots relative to whole plant. Initially, the hydraulic resistance of leaves accounted for approximately 48% of that of the whole plant. With an increase in drought duration, hydraulic resistance in leaves relative to the whole plant declined from about 48% to 13%. By contrast, hydraulic resistance in bare shoots relative to the whole plant rose from about 20% to 76%. This indicated that hydraulic contributions of both—whole roots and leaves—were slowly enhanced in drought stress (Figure 3B).

The trend in leaf-specific hydraulic conductance (expressed as hydraulic conductance per leaf area) was the same as that in hydraulic conductance. The values increased at first and then decreased with increased dryness. The values of whole roots progressively increased to the highest value at day 21 of drought, and then sharply decreased. Both values of whole shoots and the leaves arrived at the highest value at day 14 of drought. The values of the leaf in other drought treatments were higher than in CK. After 28 days of drought, the values of whole roots and whole shoots decreased 35.6% and 84.3% of that in CK, respectively (Figure 4A). Total leaf area also decreased in response to increasing drought stress, decreasing sharply until day 14 of the drought and then decreasing slightly (Figure 4B).

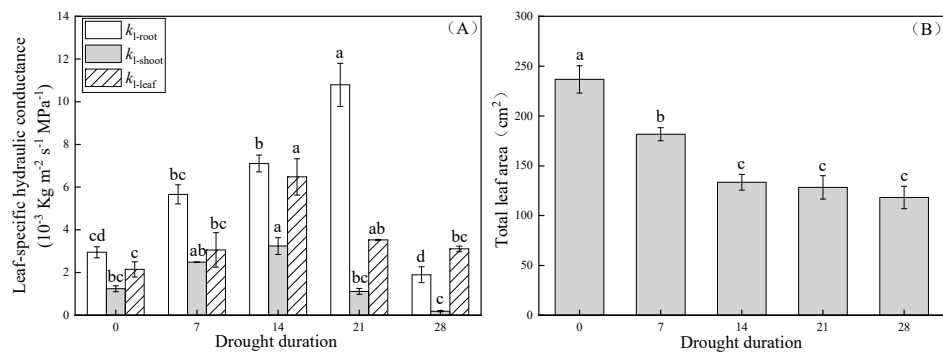


Figure 4. Changes in leaf-specific hydraulic conductance (A) and the total leaf area (B) in drought treatments. (A): k_{l-root} (open bars) indicate leaf-specific hydraulic conductance of whole roots, $k_{l-shoot}$ (light-shaded bars) indicate leaf-specific hydraulic conductance of whole shoots, k_{l-leaf} (hatched bars) indicate leaf-specific hydraulic conductance of leaves. Different lower-case letters denote significance levels based on analysis of variance (ANOVA) post hoc means with least significant difference (LSD) analysis ($p < 0.05$). Data are means with standard error.

3.2. Changes in K^+ , Mg^{+2} , Ca^+ , Malondialdehyde (MDA) Concentration and Soil Water Content

The concentration of K^+ increased sharply when drought period lasted for 7 days, decreased after 14 days, and increased again between 14 and 28 days of drought duration; all K^+ values were higher with drought than in CK. The concentration of Ca^{+2} increased in the duration of the whole drought, it increased gradually until day 14 of drought and then increased rapidly between day 14 and 28 of drought. The concentration of Mg^{+2} increased sharply until day 7 of drought, decreased until day 14, and then remained stable; Mg^{+2} concentrations during drought were higher than those in CK (Figure 5).

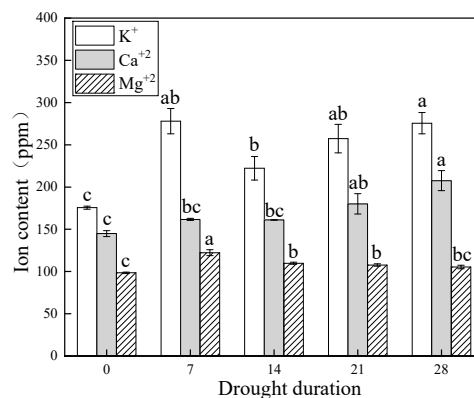


Figure 5. Changes in ion content with different durations of drought. K^+ (open bars) indicate K^+ concentrations, Ca^{+2} (light-shaded bars) indicate Ca^{+2} concentrations, Mg^{+2} (hatched bars) indicate Mg^{+2} concentrations. Different lower-case letters denote significance levels based on analysis of variance (ANOVA) post hoc means with least significant difference (LSD) analysis ($p < 0.05$). Data are means with standard error.

Soil water content declined sharply when drought lasted for 7 days, and then gradually decreased. At 28 days of drought duration, soil water content declined to about 4.5% (Figure 6A). The trend in MDA was the opposite of that of soil water content. MDA content increased gradually when drought lasted for 21 days, and then significantly increased after 28 days of drought. MDA content continued to ascend until it reached a value about two times that of CK on the 28th day of drought (Figure 6B).

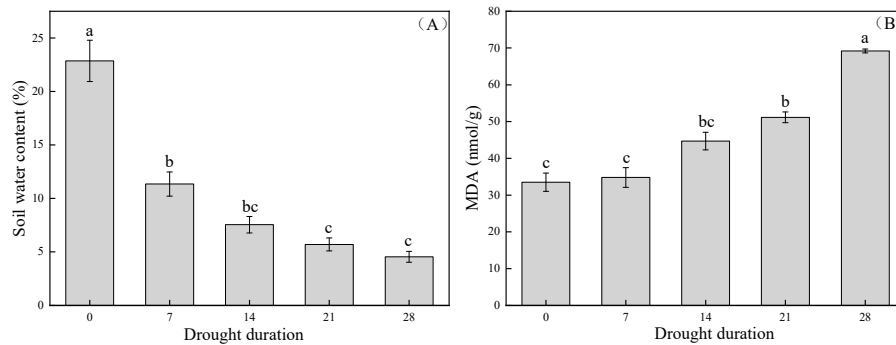


Figure 6. Changes in soil water content (A) and malondialdehyde (MDA) (B) with different durations of drought. Different lower-case letters denote significance levels based on analysis of variance (ANOVA) post hoc means with least significant difference (LSD) analysis ($p < 0.05$). Data are means with standard error.

3.3. Characteristics of Xylem Anatomy

Xylem vessels occurred singly or in small groups of two to five (Figure 7). The occurrence of vessel groups could contribute to the ionic effect which has been suggested to play a functional role in the fine regulation of xylem water transport [34]. This distribution was independent of treatment ($p > 0.05$). Diameters of vessels were largest for roots (39.53 to 46.15 μm), medium for shoots (30.3 to 37.23 μm), and smallest for leaves (13.8 to 16.05 μm). Variability in vessel diameters was the same for shoots and roots. Vessel diameters increased from 0 (CK) to 14 days of drought and then decreased slightly for day 14 to 28 of drought. Vessel diameters in leaves did not differ with treatment (Figure 8A).

Water flowed between adjacent vessels through pit connections. There were many pits in the walls of *P. euphratica* vessels which affected the horizontal water transport. Pit radius in roots gradually increased until day 14 of drought, and then gradually decreased until day 28. Pit radius in shoots did not differ among treatments (Figure 8B).

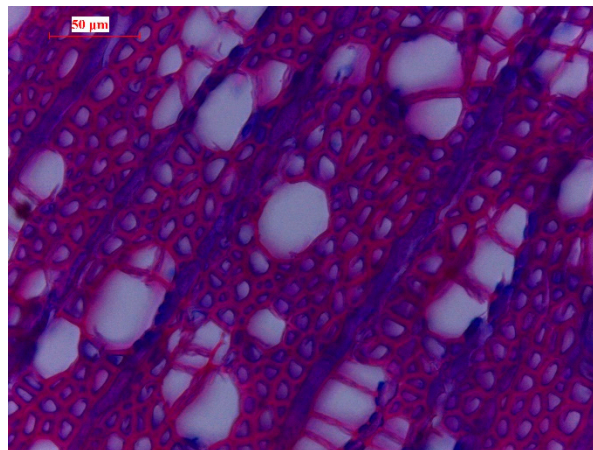


Figure 7. Microscopic images of xylem vessels in small groups in shoot cross-sections.

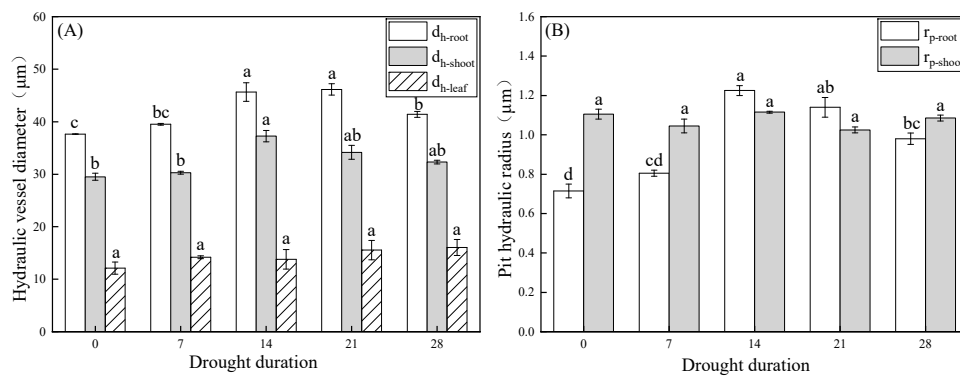


Figure 8. Vessel hydraulic diameter in xylem (A), and pit radius (B) in different drought treatments. (A): d_{h-root} (open bars) indicate vessel hydraulic diameter of the root, $d_{h-shoot}$ (light-shaded bars) indicate vessel hydraulic diameter of the shoot, d_{h-leaf} (hatched bars) indicate vessel hydraulic diameter of the leaf. (B): r_{p-root} (open bars) indicate pit radius of the root, $r_{p-shoot}$ (light-shaded bars) indicate pit radius of the shoot. Different lower-case letters denote significance levels based on analysis of variance (ANOVA) post hoc means with least significant difference (LSD) analysis ($p < 0.05$). Data are means with standard error.

The ratios of thickness-to-span initially decreased, and then increased with the increase in the duration of drought. The trends changed at the different duration of drought. Thickness-to-span ratios in roots declined for 21 days of drought and then increased. Thickness-to-span ratios of the root got to the lowest point on day 21 of drought (Figure 9A). The ratio for shoot progressively declined to the lowest value at day 14 of drought, and then slightly increased. Both thickness-to-span ratios of the shoot and the leaf arrived at the lowest point on day 14 of drought (Figure 9B,C). After the lowest point, the values went up. That is, the vessel wall reinforcement for all the parts got weakened at first, and was then enhanced after attaining the limit value.

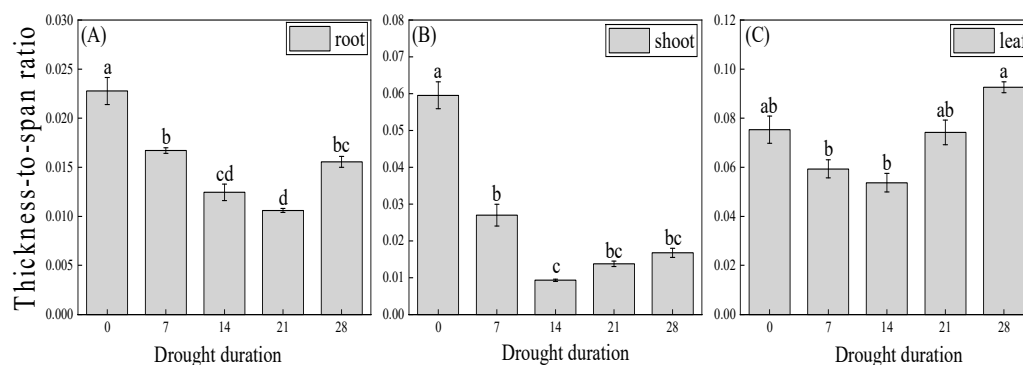


Figure 9. The thickness-to-span ratio in the xylem of *P. euphratica* without (0-days) and with drought (day 7 to 28). (A): root, (B): shoot, (C): leaf. Different lower-case letters denote significance levels based on analysis of variance (ANOVA) post hoc means with least significant difference (LSD) analysis ($p < 0.05$). Data are means with standard error.

4. Discussion

4.1. Hydraulic Conductance in Drought Conditions

Hydraulic conductance of *P. euphratica* parts (e.g., roots, shoots, leaves) was enhanced with drought stress. This provided evidence that *P. euphratica* can maintain efficient water transport, which allows it to survive in an extremely arid climate. These results were similar to those in *Pinus ponderosa*, in which long-term water transport capacity in arid areas was improved [35]. However, root hydraulic conductance of some trees was reduced under drought stress [36,37]. This was probably due to the species-specific hydraulic characteristic of plants in arid regions. Roots were vital for water transport in

drought adaptation. Roots contributed less than one-third of plant internal resistance to the whole plant hydraulic conductance. Hydraulic characteristics of *P. euphratica* roots in drought conditions tended to exhibit higher values than shoots. Previous studies showed that roots contributed 20% to 90% of the whole plant hydraulic resistance for different plants in the diverse environment [38]. This may suggest that the adjustment of the hydraulic contribution of roots was according to the living environment for different plants. With increasing drought stress, root resistance gradually decreased, and hydraulic conductance gradually increased. Stomatal conductance as the main short-term regulator of plant water flux could be affected by increased hydraulic characteristics through magnifying the hydraulic signal. *P. euphratica* could decrease water loss by adjusting stomatal conductance during suffering severe water shortage; therefore, water use efficiency was improved coupled with an increase in hydraulic capacity [16,39]. Plants enhanced water transport capacity of the leaves, which initially accounted for a substantial portion of hydraulic resistance in whole shoots. As a result, changes in leaf hydraulic conductance may have a much larger impact than those in stem [40]. In this manner, water can be relatively easily transported from stem to leaves.

Previous research suggested that a principal process controlled by hydraulic conductivity was tissue death occurring at a threshold corresponding to 80% loss of xylem leaf-specific hydraulic conductance [41–43]. Enhancement of water transport may be effective when soil water is accessible. When soil water content was much lower than the water demand for the adjustment of hydraulic characteristics, the enhancement could not be effective because the hydraulic limit was at the root ability to absorb soil water, and widespread xylem embolism due to the likely low xylem water potential at negative values. When drought duration reached 28 days in our study, xylem leaf-specific hydraulic conductance of whole shoots declined to 80% of CK. The soil moisture content of about 4.5% could lead to mortality of aboveground parts. In this study, canopy mortality occurred relatively rapidly in a severe drought. A decrease in efficiency of water transport from soil to leaves and leaf drop may result in hydraulic isolation of the shoots, that is, rendering shoots without sufficient water supply. In those conditions, leaf-specific hydraulic conductance of whole roots decreased by only about 36% and roots endured. This may explain how roots enable plants to recover from periods of drought even following the appearance of catastrophic damage to the shoots [13]. Frequent episodes of hydraulic failure that may occur in high water-stress environments could break the balance of the soil-plant-atmosphere continuum.

4.2. Vertical and Horizontal Water Transport Affect Hydraulic Conductance

Plants can absorb water from the soil then transport it vertically up through the vessels to their leaves. Vertical water transport in plants is strongly affected by vessel hydraulic diameter, which is strongly influenced by the environment [44]. Our study showed that diameters of vessels were largest for roots, medium for shoots, and smallest for leaves. Therefore, resistance to cavitation that is higher in leaves than in shoots and in roots may be interpreted as a consequence of narrower vessel diameters. Additionally, the wider vessel hydraulic diameter of roots and shoots increased in response to severe drought which showed a high vulnerability to xylem embolism in both shoots and roots. This conclusion is consistent with a previous study of *P. euphratica* [17]. Hydraulic conductance was radically affected by variability in the internal diameter of xylem vessels. The diameter of xylem vessels determines the flow rate in plants which has vital functional implications for water transport. Small increases in vessel diameter could lead to major gains in hydraulic conductance [45,46]. The adjustment of xylem vasculature aimed to maximize hydraulic conductance to efficiently deliver water to leaves in vertical water transport.

Water travels not only through vessels vertically but also by horizontal water transport through the bordered pits of vessels [47]. Pit radii in roots increased in response to severe drought, while those in shoots exhibited no significant changes; the effect of broader vessel diameter accompanied by bigger pores of pits resulted in an increase in the water transfer efficiency of roots. Pit membranes are altered by the swelling and shrinking of pectins, hydrogel properties of which are currently thought to be the

major cause of the ionic effect [48]. Hydraulic conductance of xylem is sensitive to ion concentration, increasing in response to an increase in ion concentration. The regulation of levels of specific inorganic ions could affect pore size of pits by the changes in pectins properties. A strategy that employs mainly ions to affect hydraulic conductance is energetically favorable due to resource availability and low cost [49]. Cation-mediated volume changes in pit-membrane pectins would modify the diameter of nanometer-sized pores of pits and thus change their hydraulic conductance [50]. Concentrations of the main cations (K^+ , Ca^{+2} , Mg^{+2}) were higher in leaves in all drought treatments than in CK. An increase in ion concentration which was likely induced by the re-circulation of ions prior to leaf shedding was notable as a component of possible physiological adjustment of xylem hydraulic conductance to environmental changes [51]. Several previous studies indicated the involvement of components of cell walls except for pectins as well as electrokinetic effects, which could explain the so-called ionic effect [52,53]. Cellulose microfibrils and lignins affect pit membranes in ion-mediated control of hydraulic conductance. Electrokinetic effects in plant xylem may be involved in the processes in which hydraulic conductance of an electrically-charged porous membrane varies with the properties of the electrolyte. Even though total cation concentration continued to increase with drought duration, the increase in MDA content indicated increasing stress-induced damage on pit membranes, in which the pore of the pit began to shrink as a result of the decrease in membrane elasticity.

4.3. Trade-off between Hydraulic Efficiency and Hydraulic Safety

Hydraulic efficiency of a plant is determined by hydraulic conductance, and hydraulic safety is threatened by xylem cavitation. Xylem cavitation is a plant consequence of drought stress [12]. Cavitation occurs when metastable liquid water is replaced by water vapor due to the expansion of gas bubbles, forming an embolism or air blockage that disrupts water transport [54]. Plants thus face the challenge of limiting the risk of xylem cavitation, while maintaining high xylem conductance [32,55]. Drought-induced cavitation could be brought about from air seeding via bordered pits in horizontal water transport [33]. In horizontal water transport, large pores in pit membranes facilitate water flow and enhance conductance on the one hand, but compromise cavitation containment on the other hand, and are vulnerable to air seeding [47]. In our experiment, pit radii in roots decreased after a period of increase, indicating a trade-off in pit traits through physiological changes.

Besides coming out in horizontal water transport, drought-induced cavitation could also result from vessel implosion in vertical water transport [33]. In vertical water transport, there may be a trade-off between hydraulic conductance and wall reinforcement. A functional interpretation is that the stress induced by xylem tension in the vessel wall increases with increasing vessel hydraulic diameter, leading to a trade-off between hydraulic efficiency of vessels and resistance to collapse [56]. The xylem vessel thickness-to-span ratios were thought to be predictive of collapse [57]. The thickness-to-span ratios of different plant parts in this study showed a decrease to the lowest value, the hydraulic conductance change point, then an increase. At the lowest value, the vessels may have reached the minimum xylem strength while still maintaining a high water transfer efficacy. After that point, the vessel hydraulic diameter decreased gradually; this may be attributed to xylem conduit inability to withstand the mechanical forces imposed by the negative pressure, resulting in deformation or collapse [58,59]. The consideration of hydraulic efficiency was first within the range of reaching the hydraulic safety limit for the trees. Once it went to hydraulic safety limit, hydraulic efficiency had to be reduced to bypass catastrophic xylem failure. This was an adjustment of the hydraulic efficiency of vessels and hydraulic safety to avoid leading to a catastrophic xylem failure; the adjustment reflected a trade-off between vessel construction and defense against drought-induced cavitation. Shoot dieback and tree seedling mortality were often a result of a catastrophic hydraulic failure due to cavitation in xylem vessels [60]. Our research suggests that the balance point between cavitation and hydraulic conductance from plant anatomy could be confirmed by using vessel thickness-to-span ratios as structural indicators of wall reinforcement.

5. Conclusions

The mechanism of hydraulic properties of *P. euphratica* during drought was studied based on analysis of whole root, whole shoot, and leaves in tree seedlings. *P. euphratica* enhanced hydraulic transport during severe drought stress before the soil water content dropped to a threshold. Drought-induced loss of hydraulic conductance could impair water transport capacity of plants when the soil water content overcame to the threshold; the threshold of soil water content in the rhizosphere for the survival of roots was higher than that of the overground parts. Crown mortality occurred when the soil water content in the rhizosphere got to the threshold for the overground parts. Research on horizontal and vertical water transport in *P. euphratica* increased the understanding of internal mechanisms of drought acclimation. Our results highlight the critical importance of anatomical and physiological changes in influencing hydraulic characteristics of trees in contrasting drought response strategies. Furthermore, we also found that there was a crucial point in the tradeoffs between hydraulic efficiency. The consideration of hydraulic efficiency was first within the range of reaching the hydraulic safety limit. Once the hydraulic safety limit was reached, safety would be taken as the first consideration and hydraulic efficiency would be reduced. Further understanding of the trade-off between hydraulic efficiency and hydraulic safety accompanied by the soil water content threshold will improve predictions of plant and ecosystem water use in response to severe drought stress.

Author Contributions: D.L. and J.S. collected experimental data, analyzed, and wrote the manuscript. Other co-authors participated equally in conceptualization, data analysis, and manuscript preparation and review.

Funding: This research was funded by the National Key R&D Program of China (No.2016YFC0400908, 2016YFC0501009), Major Science and Technology Project in Inner Mongolia Autonomous Region (zdzx2018057) and Chinese Academy of Sciences Innovative Cross Team Project (JCTD-2019-19).

Acknowledgments: Thanks to Kathryn B. Piatek for her editorial suggestions. The authors sincerely appreciate the helpful and constructive comments made by reviewers of the draft manuscript.

Conflicts of Interest: The authors declare no conflicts of interest.

References

- Engelbrecht, B.M.; Comita, L.S.; Condit, R.; Kursar, T.A.; Tyree, M.T.; Turner, B.L.; Hubbell, S.P. Drought sensitivity shapes species distribution patterns in tropical forests. *Nature* **2007**, *447*, 80–82. [[CrossRef](#)] [[PubMed](#)]
- Cochard, H.; Barigah, S.T.; Kleinhentz, M.; Eshel, A. Is xylem cavitation resistance a relevant criterion for screening drought resistance among *Prunus* species? *J. Plant Physiol.* **2008**, *165*, 976–982. [[CrossRef](#)] [[PubMed](#)]
- Ennajeh, M.; Tounekti, T.; Vadel, A.M.; Khemira, H.; Cochard, H. Water relations and drought-induced embolism in olive (*Olea europaea*) varieties ‘Meski’ and ‘Chemlali’ during severe drought. *Tree Physiol.* **2008**, *28*, 971–976. [[CrossRef](#)] [[PubMed](#)]
- Fan, D.Y.; Xie, Z.Q. Several controversial viewpoints in studying the cavitation of xylem vessels. *Acta Phytoecol. Sin.* **2004**, *28*, 126–132.
- Chen, Y.; Chen, Y.; Xu, C.; Li, W. Groundwater depth affects the daily course of gas exchange parameters of *Populus euphratica* in arid areas. *Environ. Earth Sci.* **2012**, *66*, 433–440. [[CrossRef](#)]
- Si, J.; Feng, Q.; Cao, S.; Yu, T.; Zhao, C. Water use sources of desert riparian *Populus euphratica* forests. *Environ. Monit. Assess.* **2014**, *186*, 5469–5477. [[CrossRef](#)]
- Sack, L.; Tyree, M.T.; Holbrook, N.M. Leaf hydraulic architecture correlates with regeneration irradiance in tropical rainforest trees. *New Phytol.* **2005**, *167*, 403–413. [[CrossRef](#)]
- Meinzer, F.C. Co-ordination of vapour and liquid phase water transport properties in plants. *Plant Cell Environ.* **2002**, *25*, 265–274. [[CrossRef](#)]
- Cochard, H. Vulnerability of several conifers to air embolism. *Tree Physiol.* **1992**, *11*, 73–83. [[CrossRef](#)]
- Willson, C.J.; Jackson, R.B. Xylem cavitation caused by drought and freezing stress in four co-occurring *Juniperus* species. *Physiol. Plant.* **2006**, *127*, 374–382. [[CrossRef](#)]

11. Urli, M.; Porté, A.J.; Cochard, H.; Guengant, Y.; Burlett, R.; Delzon, S. Xylem embolism threshold for catastrophic hydraulic failure in angiosperm trees. *Tree Physiol.* **2013**, *33*, 672–683. [[CrossRef](#)] [[PubMed](#)]
12. Ladjal, M.; Huc, R.; Ducrey, M. Drought effects on hydraulic conductivity and xylem vulnerability to embolism in diverse specie and provenances of Mediterranean cedars. *Tree Physiol.* **2005**, *25*, 1109. [[CrossRef](#)] [[PubMed](#)]
13. Anderegg, W.R.L.; Anderegg, L.D.L. Hydraulic and carbohydrate changes in experimental drought-induced mortality of saplings in two conifer species. *Tree Physiol.* **2013**, *33*, 252–260. [[CrossRef](#)] [[PubMed](#)]
14. Sun, C.; Gao, X.; Chen, X.; Fu, J.; Zhang, Y. Metabolic and growth responses of maize to successive drought and re-watering cycles. *Agric. Water Manag.* **2016**, *172*, 62–73. [[CrossRef](#)]
15. Sperry, J.S.; Hacke, U.G.; Oren, R.; Comstock, J.P. Water deficits and hydraulic limits to leaf water supply. *Plant Cell Environ.* **2010**, *25*, 251–263. [[CrossRef](#)]
16. Li, D.; Si, J.; Zhang, X.; Gao, Y.; Wang, C.; Luo, H.; Qin, J.; Gao, G. Hydraulic characteristics of *Populus euphratica* in an arid environment. *Forests* **2019**, *10*, 407. [[CrossRef](#)]
17. Hukin, D.; Cochard, H.; Dreyer, E.; Thiec, D.L.; Bogeat-Triboulot, M.B. Cavitation vulnerability in roots and shoots: Does *Populus euphratica* Oliv., a poplar from arid areas of Central Asia, differ from other poplar species? *J. Exp. Bot.* **2005**, *56*, 2003–2010. [[CrossRef](#)]
18. Zhou, H.; Chen, Y.; Li, W.; Ayup, M. Xylem hydraulic conductivity and embolism in riparian plants and their responses to drought stress in desert of Northwest China. *Ecohydrology* **2013**, *6*, 984–993. [[CrossRef](#)]
19. Pan, Y.; Chen, Y.; Chen, Y.; Wang, R.; Ren, Z. Impact of groundwater depth on leaf hydraulic properties and drought vulnerability of *Populus euphratica* in the Northwest of China. *Trees* **2016**, *30*, 2029–2039. [[CrossRef](#)]
20. Vandersande, M.W.; Glenn, E.P.; Walworth, J.L. Tolerance of five riparian plants from the lower Colorado River to salinity drought and inundation. *J. Arid Environ.* **2001**, *49*, 147–159. [[CrossRef](#)]
21. Chen, Y.; Li, W.; Chen, Y.; Zhang, H.; Zhuang, L. Physiological response of natural plants to the change of groundwater level in the lower reaches of Tarim River, Xinjiang. *Prog. Nat. Sci.* **2004**, *14*, 975–983. [[CrossRef](#)]
22. Chen, Y.; Chen, Y.; Xu, C.; Li, W. Photosynthesis and water use efficiency of *Populus euphratica* in response to changing groundwater depth and CO₂ concentration. *Environ. Earth Sci.* **2011**, *62*, 119–125. [[CrossRef](#)]
23. Martre, P.; Morillon, R.; Barrieu, F.; North, G.B.; Nobel, P.S.; Chrispeels, M.J. Plasma membrane aquaporins play a significant role during recovery from water deficit. *Plant Physiol.* **2002**, *130*, 2101–2110. [[CrossRef](#)] [[PubMed](#)]
24. Si, J.H.; Chang, Z.Q.; Su, Y.H.; Xi, H.Y.; Feng, Q. Stomatal conductance characteristics of *Populus euphratica* leaves and response to environmental factors in the extreme arid region. *Acta Bot. Boreali-Occident. Sin.* **2008**, *11*, 1596–1599.
25. Tyree, M.T.; Patiño, S.; Bennink, J.; Alexander, J. Dynamic measurements of roots hydraulic conductance using a high-pressure flowmeter in the laboratory and field. *J. Exp. Bot.* **1995**, *46*, 83–94. [[CrossRef](#)]
26. Sack, L.; Melcher, P.J.; Zwieniecki, M.A.; Holbrook, N.M. The hydraulic conductance of the angiosperm leaf lamina: A comparison of three measurement methods. *J. Exp. Bot.* **2002**, *53*, 2177–2184. [[CrossRef](#)]
27. Raimondo, F.; Trifilo, P.; Gullo, M.L.; Buffa, R.; Nardini, A.; Salleo, S. Effects of reduced irradiance on hydraulic architecture and water relations of two olive clones with different growth potentials. *Environ. Exp. Bot.* **2009**, *66*, 249–256. [[CrossRef](#)]
28. Alsina, M.M.; Smart, D.R.; Bauerle, T.; De Herralde, F.; Biel, C.; Stockert, C.; Negron, C.; Save, R. Seasonal changes of whole root system conductance by a drought-tolerant grape root system. *J. Exp. Bot.* **2010**, *62*, 99–109. [[CrossRef](#)]
29. Han, X.; He, X.; Qiu, W.; Lu, Z.; Zhang, Y.; Chen, S.; Liu, M.; Qiao, G.; Zhuo, R. Pathogenesis-related protein PR10 from *Salix matsudana* Koidz exhibits resistance to salt stress in transgenic *Arabidopsis thaliana*. *Environ. Exp. Bot.* **2017**, *141*, 74–82. [[CrossRef](#)]
30. Jacobsen, A.L.; Agenbag, L.; Esler, K.J.; Pratt, R.B.; Ewers, F.W.; Davis, S.D. Xylem density, biomechanics and anatomical traits correlate with water stress in 17 evergreen shrub species of the Mediterranean-type climate region of South Africa. *J. Ecol.* **2007**, *95*, 171–183. [[CrossRef](#)]
31. Zimmermann, M.H. *Xylem Structure and the Ascent of Sap*; Springer: Berlin, Germany, 2013.
32. Pittermann, J.; Sperry, J.S.; Wheeler, J.K.; Hacke, U.G.; Sikkema, E.H. Mechanical reinforcement of tracheids compromises the hydraulic efficiency of conifer xylem. *Plant Cell Environ.* **2006**, *29*, 1618–1628. [[CrossRef](#)] [[PubMed](#)]

33. Hacke, U.G.; Sperry, J.S.; Pockman, W.T.; Davis, S.D.; McCulloh, K.A. Trends in wood density and structure are linked to prevention of xylem implosion by negative pressure. *Oecologia* **2001**, *126*, 457–461. [[CrossRef](#)]
34. Jansen, S.; Gortan, E.; Lens, F.; Lo Gullo, M.A.; Salleo, S.; Scholz, A.; Stein, A.; Trifilò, P.; Nardini, A. Do quantitative vessel and pit characters account for ion-mediated changes in the hydraulic conductance of angiosperm xylem? *New Phytol.* **2011**, *189*, 218–228. [[CrossRef](#)] [[PubMed](#)]
35. Maherali, H.; DeLucia, E.H. Xylem conductivity and vulnerability to cavitation of ponderosa pine growing in contrasting climates. *Tree Physiol.* **2000**, *20*, 859–867. [[CrossRef](#)] [[PubMed](#)]
36. Tabassum, M.A.; Ye, Y.; Yu, T.; Zhu, G.; Rizwan, M.S.; Wahid, M.A.; Peng, S.; Li, Y. Rice (*Oryza sativa* L.) hydraulic conductivity links to leaf venation architecture under well-watered condition rather than PEG-induced water deficit. *Acta Physiol. Plant.* **2016**, *38*, 1–11. [[CrossRef](#)]
37. Limousin, J.M.; Longepierre, D.; Huc, R.; Rambal, S. Change in hydraulic traits of Mediterranean *Quercus ilex* subjected to long-term throughfall exclusion. *Tree Physiol.* **2010**, *30*, 1026–1036. [[CrossRef](#)] [[PubMed](#)]
38. Tsuda, M.; Tyree, M.T. Whole-plant hydraulic resistance and vulnerability segmentation in *Acer saccharinum*. *Tree Physiol.* **1997**, *17*, 351–357. [[CrossRef](#)]
39. Li, J.Y.; Zhao, C.Y.; Li, J.; Yan, Y.Y.; Yu, B.; Han, M. Growth and leaf gas exchange in *Populus euphratica* across soil water and salinity gradients. *Photosynthetica* **2013**, *51*, 321–329. [[CrossRef](#)]
40. Nardini, A.; Salleo, S.; Raimondo, F. Changes in leaf hydraulic conductance correlate with leaf vein embolism in *Cercis siliquastrum* L. *Trees* **2003**, *17*, 529–534. [[CrossRef](#)]
41. Tyree, M.T.; Engelbrecht, B.M.; Vargas, G.; Kursar, T.A. Desiccation tolerance of five tropical seedlings in Panama. Relationship to a field assessment of drought performance. *Plant Physiol.* **2003**, *132*, 1439–1447. [[CrossRef](#)]
42. Tyree, M.T.; Vargas, G.; Engelbrecht, B.M.; Kursar, T.A. Drought until death do us part: A case study of the desiccation-tolerance of a tropical moist forest seedling-tree, *Licania platypus* (Hemsl.) Fritsch. *J. Exp. Bot.* **2002**, *53*, 2239–2247. [[CrossRef](#)] [[PubMed](#)]
43. Kursar, T.A.; Engelbrecht, B.M.; Burke, A.; Tyree, M.T.; El Omari, B.; Giraldo, J.P. Tolerance to low leaf water status of tropical tree seedlings is related to drought performance and distribution. *Funct. Ecol.* **2009**, *23*, 93–102. [[CrossRef](#)]
44. Jacobsen, A.L.; Pratt, R.B.; Tobin, M.F.; Hacke, U.G.; Ewers, F.W. A global analysis of xylem vessel length in woody plants. *Am. J. Bot.* **2012**, *99*, 1583–1591. [[CrossRef](#)] [[PubMed](#)]
45. Cruiziat, P.; Cochard, H.; Améglio, T. Hydraulic architecture of trees: Main concepts and results. *Ann. For. Sci.* **2002**, *59*, 723–752. [[CrossRef](#)]
46. McElrone, A.J.; Pockman, W.T.; Martínez-Vilalta, J.; Jackson, R.B. Variation in xylem structure and function in stems and roots of trees to 20 m depth. *New Phytol.* **2004**, *163*, 507–517. [[CrossRef](#)]
47. Hacke, U.G.; Sperry, J.S. Functional and ecological xylem anatomy. *Perspect. Plant Ecol. Evol. Syst.* **2001**, *4*, 97–115. [[CrossRef](#)]
48. Zwieniecki, M.A.; Melcher, P.J.; Holbrook, N.M. Hydrogel control of xylem hydraulic resistance in plants. *Science* **2001**, *291*, 1059–1062. [[CrossRef](#)]
49. Ottow, E.A.; Brinker, M.; Teichmann, T.; Fritz, E.; Kaiser, W.; Brosché, M.; Kangasjärvi, J.; Jiang, X.; Polle, A. *Populus euphratica* displays apoplastic sodium accumulation, osmotic adjustment by decreases in calcium and soluble carbohydrates, and develops leaf succulence under salt stress. *Plant Physiol.* **2005**, *139*, 1762–1772. [[CrossRef](#)]
50. Nardini, A.; Salleo, S.; Jansen, S. More than just a vulnerable pipeline: Xylem physiology in the light of ion-mediated regulation of plant water transport. *J. Exp. Bot.* **2011**, *62*, 4701–4718. [[CrossRef](#)]
51. Aasamaa, K.; Söber, A. Sensitivity of stem and petiole hydraulic conductance of deciduous trees to xylem sap ion concentration. *Biol. Plant.* **2010**, *54*, 299–307. [[CrossRef](#)]
52. Herbette, S.; Bouchet, B.; Brunel, N.; Bonnin, E.; Cochard, H.; Guillon, F. Immunolabelling of intervessel pits for polysaccharides and lignin helps in understanding their hydraulic properties in *Populus tremula* × *alba*. *Ann. Bot.* **2014**, *115*, 187–199. [[CrossRef](#)] [[PubMed](#)]
53. Santiago, M.; Pagay, V.; Stroock, A.D. Impact of electroviscosity on the hydraulic conductance of the bordered pit membrane: A theoretical investigation. *Plant Physiol.* **2013**, *163*, 999–1011. [[CrossRef](#)] [[PubMed](#)]
54. Lens, F.; Tixier, A.; Cochard, H.; Sperry, J.S.; Jansen, S.; Herbette, S. Embolism resistance as a key mechanism to understand adaptive plant strategies. *Curr. Opin. Plant Biol.* **2013**, *16*, 287–292. [[CrossRef](#)] [[PubMed](#)]

55. Hacke, U.G.; Sperry, J.S.; Wheeler, J.K.; Castro, L. Scaling of angiosperm xylem structure with safety and efficiency. *Tree Physiol.* **2006**, *26*, 689–701. [[CrossRef](#)]
56. Zhang, Y.J.; Rockwell, F.E.; Graham, A.C.; Alexander, T.; Holbrook, N.M. Reversible leaf xylem collapse: A potential “circuit breaker” against cavitation. *Plant Physiol.* **2016**, *172*, 2261–2274. [[CrossRef](#)]
57. Blackman, C.J.; Brodribb, T.J.; Jordan, G.J. Leaf hydraulic vulnerability is related to conduit dimensions and drought resistance across a diverse range of woody angiosperms. *New Phytol.* **2010**, *188*, 1113–1123. [[CrossRef](#)]
58. Brodribb, T.J. Water Stress Deforms Tracheids Peripheral to the Leaf Vein of a Tropical Conifer. *Plant Physiol.* **2005**, *137*, 1139–1146. [[CrossRef](#)]
59. Zhang, Y.J.; Rockwell, F.E.; Wheeler, J.K.; Holbrook, N.M. Reversible Deformation of Transfusion Tracheids in *Taxus baccata* Is Associated with a Reversible Decrease in Leaf Hydraulic Conductance. *Plant Physiol.* **2014**, *165*, 1557. [[CrossRef](#)]
60. Davis, S.D.; Ewers, F.W.; Sperry, J.S.; Portwood, K.A.; Crocker, M.C.; Adams, G.C. Shoot dieback during prolonged drought in *Ceanothus* (Rhamnaceae) chaparral of California: A possible case of hydraulic failure. *Am. J. Bot.* **2002**, *89*, 820–828. [[CrossRef](#)]



© 2019 by the authors. Licensee MDPI, Basel, Switzerland. This article is an open access article distributed under the terms and conditions of the Creative Commons Attribution (CC BY) license (<http://creativecommons.org/licenses/by/4.0/>).